Phase Transformations Involving Network Phases in ISO Triblock Copolymer−Homopolymer Blends

Thomas H. Epps, III,† Joon Chatterjee, and Frank S. Bates*

Department of Chemical Engineering and Materials Science, University of Minnesota, Minneapolis, Minnesota 55455

Received April 8, 2005; Revised Manuscript Received August 4, 2005

ABSTRACT: Poly(isoprene-*b*-styrene-*b*-ethylene oxide) (ISO) triblock copolymers were blended with poly(styrene) and poly(isoprene) homopolymers at compositions close to those previously shown to produce triply periodic, multiply continuous network phases. Homopolymer molecular weights were approximately equal to the corresponding block molecular weights, and homopolymer concentrations up to 21 vol % were explored without evidence of phase separation. Three triply periodic network phases were identified: a core−shell double gyroid (Q^{230}, $Ia\bar{3}d$ space group symmetry), an orthorhombic network (O^{70}, *Fddd* space group symmetry), and an alternating gyroid (Q^{214}, $I4_132$ space group symmetry). Tuning the overall composition by adding homopolymer resulted in systematic phase transitions between the Q^{230} and O^{70} networks and between the Q^{214} and O^{70} networks. In addition, doping with both poly(styrene) and poly(isoprene) homopolymer induced transitions from three-domain lamellae (LAM_3) to the O^{70} network phase. In general, phases identified in the triblock/homopolymer systems are located at nearly the same compositions established for undiluted ISO. Specific structural assignments and qualitative assessments of long-range order were made using small-angle X-ray scattering (SAXS), birefringence, dynamic mechanical spectroscopy (DMS), and transmission electron microscopy (TEM) data acquired from polydomain (powdered) samples. The results presented herein demonstrate an efficient method for exploring triblock copolymer phase space based on precise and continuous composition control.

I. Introduction

Network structures in block copolymers present exciting opportunities to exploit nanoscale self-assembly in practical ways. Morphologies that combine three-dimensional continuity and periodicity offer many possible commercial applications in areas such as membranes, optical communications, electrical and ionic conductors, nanotemplating, and nanolithography.[1−7] During the past decade the double gyroid structure (Q^{230}) was identified in AB diblocks,[8−12] and at least three network phases have been reported in ABC triblock copolymer melts: the pentacontinuous core−shell gyroid (Q^{230}),[13−15] the triply continuous alternating gyroid (Q^{214}),[16,17] and the orthorhombic O^{70} phase.[18−21] Self-consistent mean-field theory has corroborated these experimental findings, predicting a band of three equilibrium network states (Q^{230}, O^{70}, and Q^{214}) at compositions between those associated with two-domain and three-domain lamellae.[22] Establishing these experimental and theoretical facts required an extensive synthetic and characterization effort. This paper describes an alternative strategy for maneuvering between these structures with minimal investment in polymer synthesis.

In previous publications we reported the detailed characterization of a series of poly(isoprene-*b*-styrene-*b*-ethylene oxide) (ISO) triblock copolymers.[19−21] A two-step anionic polymerization technique provided a convenient and relatively efficient method for preparing families of triblocks along compositional isopleths with precise control over composition and molecular weight.[19,23] However, establishing phase behavior in these complex materials, particularly locating boundaries between phase states, was a tedious and time-consuming process, requiring the synthesis of numerous samples along closely spaced isopleths. Polymer blending presents a more efficient method for microstructure exploration, obviating the need for extensive synthesis, while simultaneously providing continuous and precise control over composition.

Blending homopolymers with diblock copolymers represents a well-established technique for controlling morphology. All phases found in pure AB diblock and ABA triblock copolymers (lamellae, cylinders, spheres, perforated structures, and network structures) have been identified in diblock/homopolymer and triblock/homopolymer blends.[24−34] In some cases sufficient amounts of homopolymer have led to phases not found in the corresponding neat (undiluted) block copolymers, and calculations by Matsen have shown that homopolymer can stabilize certain new morphologies.[26] Doping with homopolymer also can lead to macroscopic phase separation, depending on the overall block and homopolymer molecular weights and composition.[24,30,35−39]

The mixing patterns in homopolymer/diblock copolymer systems are conveniently summarized in three categories based on the ratio ($N_{h,A}/N_{b,A}$), where $N_{h,A}$ and $N_{b,A}$ refer to the degree of polymerization of A homopolymer and the degree of polymerization of the A block, respectively.[40,41] When $N_{h,A}/N_{b,A} < 1$, homopolymer swells the corresponding block, a situation often referred to as a "wet brush". Increasing the homopolymer molecular weight to $N_{h,A}/N_{b,A} \approx 1$ leads to expulsion of the homopolymer from the brush interior and localization of the homopolymer at the central portion of the microdomain; this is known as the "dry brush limit". When $N_{h,A}/N_{b,A} \gg 1$, the homopolymer is rejected from the block copolymer altogether, a condition known as macrophase separation. Blending homopolymer with

† Current address: NIST−Polymers Division, 100 Bureau Drive, MS 8542, Gaithersburg, MD 20899-8542.

* To whom correspondence should be addressed.

10.1021/ma050736m CCC: $30.25
Published on Web 09/24/2005

Table 1. Neat Polymer Characterization Data[21]

polymers[a]	M_n (g/mol)	PDI	f_I	f_S	f_O	phase[b]
			Homopolymers			
PS	5 500	1.02	0.00	1.00	0.00	
PI	6 500	1.03	1.00	0.00	0.00	
			Triblocks			
ISO-1a	19 400	1.07	0.32	0.51	0.17	Q^{214}
ISO-1b	20 400	1.07	0.32	0.50	0.18	$Q^{214} \rightarrow O^{70}$
ISO-1c	22 200	1.07	0.30	0.46	0.24	O^{70}
ISO-1g	22 300	1.08	0.30	0.45	0.25	O^{70}
ISO-2a	15 400	1.07	0.49	0.36	0.15	Q^{230}
ISO-2b	16 300	1.07	0.46	0.34	0.20	Q^{230}
ISO-3f	16 300	1.05	0.42	0.43	0.15	O^{70}
ISO-3g	16 900	1.06	0.41	0.41	0.18	O^{70}
ISO-3h	17 100	1.05	0.41	0.41	0.18	O^{70}
ISO-3i	17 800	1.06	0.39	0.40	0.21	O^{70}
ISO-3k	19 400	1.06	0.36	0.37	0.27	LAM_3
ISO-3l	20 400	1.05	0.35	0.35	0.30	LAM_3
ISO-8d	20 700	1.05	0.55	0.27	0.18	CSC
ISO-15a	14 500	1.05	0.27	0.56	0.17	Q^{214}
ISO-15b	16 700	1.04	0.25	0.53	0.22	$Q^{214} \rightarrow O^{70}$
ISO-15e	18 400	1.06	0.22	0.49	0.29	$Q^{214} \rightarrow O^{70}$
ISO-15f	18 900	1.07	0.21	0.48	0.31	LAM_3
ISO-16d	16 500	1.06	0.35	0.44	0.21	O^{70}

[a] Unit cell constants and OOT/ODT data for the neat triblock copolymers can be found in previous work.[21] [b] Neat triblock ISO-8d was not examined in previous work[21] and is tentatively assigned a hexagonally packed core−shell cylindrical structure (CSC) based upon synchrotron X-ray scattering data (not shown).

ABC triblock copolymers is more complicated since the center B blocks necessarily bridge the A and C domains, thereby excluding uniform transverse separation of homopolymer to the center of the B domains; the A and C end blocks should behave like diblocks.

This study deals with the intermediate brush regime. ISO triblock copolymers have been blended with I and S homopolymers of approximately equal molecular weight to the corresponding blocks. We have examined the selective dilution of I end blocks, S middle blocks, and I + S end and middle blocks simultaneously. Our goal is to determine the feasibility of inducing transitions between ordered phases, particularly network phases. The choice of $N_{h,A} \approx N_{b,A}$ and relatively low volume fraction loadings of homopolymer ($f_H < 0.21$) favors uniform mixing and avoidance of macroscopic phase separation.

We recently reported that the central portion of the neat ISO phase portrait, located between regions of two-domain and three-domain lamellae, contains three network phases (Q^{230}, O^{70}, and Q^{214}) each formed from 10-fold loops of trivalent connectors. In this work we examine the relative stability of these network phases when the overall I, S, and O compositions are modified by the addition of I and/or S homopolymer. Small-angle X-ray scattering (SAXS), transmission electron microscopy (TEM), dynamic mechanical spectroscopy (DMS), and birefringence measurements lead us to conclude that adjacent phases in the neat ISO phase portrait can be accessed by addition of homopolymer. These findings demonstrate that detailed mapping of ABC triblock copolymer phase behavior can be facilitated by judicious blending of homopolymer.

II. Experimental Section

Synthesis and Characterization. ISO triblock copolymers were synthesized using sequential anionic polymerization techniques, beginning with the polymerization of a sizable amount (ca. 100 g) of hydroxyl-terminated poly(isoprene-*b*-styrene) diblock copolymer. Portions of this parent polymer were reinitiated with potassium naphthalenide and reacted with varying amounts ethylene oxide monomer, resulting in a series of ISO triblocks along a compositional isopleth with constant f_S/f_I.[19,23] Block copolymer compositions (segment mole fractions) were determined by ^{1}H NMR, and block volume fractions (f_I, f_S, and f_O) were calculated on the basis of published homopolymer densities at 140 °C ($\rho_I = 0.830$, $\rho_S = 0.969$, $\rho_O = 1.064$ in g/cm^3).[42]

Molecular weights and polydispersity indices (PDIs) were determined using high-performance size exclusion chromatography (SEC) with Phenomenex Phenogel columns coupled to a Wyatt Dawn DSP laser photometer using detectors at 18 angles and a Wyatt differential refractometer. Triblock copolymer volume fractions and molecular weights are listed in Table 1.

Poly(isoprene) and poly(styrene) homopolymers were synthesized using conventional anionic polymerization techniques[43] and terminated with acidic methanol; molecular weights and PDIs are given in Table 1.

Block Copolymer/Homopolymer Blending. Measured amounts (by weight) of homopolymer and triblock copolymer were dissolved in THF. Samples were freeze-dried to constant weight in 10 mL vials and stored under argon prior to use. Up to 21 vol % hompolymer was used in preparing these mixtures.

Small-Angle X-ray Scattering (SAXS). SAXS experiments were conducted at the University of Minnesota Institute of Technology (IT) characterization facility. $\lambda = 1.54$ Å Cu Kα X-rays were generated using a Rigaku RU-200BVH rotating anode equipped with a 0.2 × 2 mm^2 microfocus cathode, total reflecting Franks mirror optics, and a nickel foil filter. Data were collected by a Siemens HI-STAR multiwire area detector located at a sample-to-detector distance of 230 cm. The beam size was approximately 1 × 1 mm, and acquisition times typically ranged from 10 to 30 min. SAXS data were corrected for detector response characteristics and plotted as scattering intensity vs the magnitude of the scattering vector, $q = 4\pi\lambda^{-1}\sin(\theta/2)$, where θ is the scattering angle. These results are referred to as IT-SAXS data.

Synchrotron SAXS experiments were conducted on the DND-CAT at the Advanced Photon Source (Argonne National Laboratory) with $\lambda = 0.827$ Å. The sample-to-detector distance was 501 cm, and data were acquired on a Mar CCD area detector. The beam-size was approximately 1 × 1 mm, and acquisition times ranged from 1 to 3 s. Sample temperature was controlled using a liquid nitrogen-cooled DSC chamber under a helium purge. Polymer specimens were heated to 200 °C (above T_{ODT} when possible) to minimize the effects of

Table 2. Triblock/Homopolymer Blending Data

polymer blend	triblock	homopolymer		blend composition			phase	T_{ODT} (T_{OOT}), °C[b,c]
		type	$f_{homopolymer}$	f_I[a]	f_S[a]	f_O[a]		
B1	ISO-2a	S	0.117	0.43	0.44	0.13	O^{70}	166
B2	ISO-2a	S	0.027	0.48	0.38	0.14	Q^{230}	>200
B3	ISO-2b	S	0.028	0.46	0.34	0.20	Q^{230}	>200
B4	ISO-2b	S	0.033	0.45	0.36	0.19	O^{70}	>200
B5	ISO-2b	S	0.046	0.44	0.37	0.19	O^{70}	>200
B6	ISO-2b	S	0.062	0.44	0.38	0.18	O^{70}	263
B7	ISO-2b	S	0.084	0.43	0.39	0.18	O^{70}	>200
B8	ISO-2b	S	0.094	0.42	0.40	0.18	O^{70}	>200
B9	ISO-2b	S	0.111	0.41	0.42	0.17	O^{70}	193
B10	ISO-3f	I	0.104	0.49	0.38	0.13	Q^{230}	180−190
B11	ISO-3g	I	0.109	0.48	0.36	0.16	Q^{230}	>200
B12	ISO-3h	I	0.111	0.47	0.35	0.18	Q^{230}	>200
B13	ISO-3i	I	0.114	0.46	0.33	0.21	Q^{230}	>200
B14	ISO-1a	I	0.146	0.43	0.43	0.14	O^{70}	160
B15	ISO-8d	S	0.122	0.48	0.36	0.16	Q^{230}	>200
B16	ISO-8d	S	0.208	0.45	0.41	0.14	Q^{230}	173
B17	ISO-15a	I	0.054	0.31	0.53	0.16	Q^{214}	160
B18	ISO-16d	S	0.174	0.29	0.54	0.17	Q^{214}	147
B19	ISO-1a	S	0.088	0.30	0.55	0.15	Q^{214}	140−150
B20	ISO-1b	S	0.073	0.30	0.54	0.16	Q^{214}	151
B21	ISO-1c	S	0.130	0.26	0.54	0.20	$O^{70} \rightarrow Q^{230*}$	172 (140)
B22	ISO-1g	S	0.090	0.27	0.51	0.22	$O^{70} \rightarrow Q^{230*}$	177 (148)
B23	ISO-15a	S	0.159	0.23	0.63	0.14	DIS	<100
B24	ISO-15b	S	0.128	0.22	0.59	0.19	DIS	<100
B25	ISO-15e	S	0.099	0.20	0.54	0.26	$Q^{214} \rightarrow O^{70}$	135 (107)
B26	ISO-15f	S	0.107	0.19	0.54	0.27	$O^{70} \rightarrow Q^{230*}$	>200 (143)
B27	ISO-3k	S/I	0.076/0.068	0.34	0.40	0.26	O^{70}	>250
B28	ISO-3l	S/I	0.103/0.102	0.34	0.39	0.27	O^{70}	>250

[a] Volume fractions calculated from homopolymer densities at 140 °C (ρ_{PI} = 0.830 g/cm^3, ρ_{PS} = 0.969 g/cm^3, ρ_{PEO} = 1.064 g/cm^3).[42] [b] Single value transition temperatures were determined by DMS; the values given as ranges were determined by IT-SAXS data taken in 10 °C increments. [c] The maximum temperature accessible on the IT-SAXS instrument was 200 °C.

thermal history and then cooled to the desired temperature. Data acquired at the synchrotron are identified as APS-SAXS. APS-SAXS and IT-SAXS specimens used identical Kapton windows and had similar polymer sample thicknesses.

Transmission Electron Microscopy (TEM). TEM micrographs were collected on a JEOL 1210 TEM operating at 120 kV, at the University of Minnesota IT Characterization Facility. Samples (50−100 nm thickness) were prepared on a Reichert cryo-ultramicrotome using a Microstar diamond knife at −60 to −90 °C. Electron contrast was achieved by preferential staining the I-domains through exposure to the vapors of a 4% aqueous solution of OsO_4 for ∼5 min. Microscopy samples were prepared from specimens previously evaluated on the SAXS apparatus, thus allowing for a direct comparison between scattering data and TEM micrographs. Samples were stored in a vacuum oven at room temperature and microtomed within 12 h of removal from the SAXS apparatus.

Static Birefringence. Birefringence measurements were conducted on 1 mm thick samples sealed under argon between two glass disks separated by an aluminum spacer. Samples were placed in a chamber between crossed polarizers and illuminated with a 5 mW HeNe laser while being heated, or cooled, at 1 °C/min using an electrically heated copper block. Transmitted depolarized light intensity was measured using a photodiode connected to a voltmeter and normalized by the detector response I_{max} recorded with the polarizers in the parallel orientation.

Dynamic Mechanical Spectroscopy (DMS). Mechanical spectroscopy experiments were performed on a Rheometrics Scientific ARES strain-controlled rheometer using a parallel plate configuration with 25 mm diameter plates. Samples were 1 mm thick. Isochronal (ω = 1 rad/s) dynamic elastic (G') and loss (G'') moduli measurements were collected during heating or cooling at 1 °C/min. For all measurements the strain amplitude was 1%, well within the linear viscoelastic regime. Data acquisition was preceded by heating to disorder or 250 °C, whichever was lower, to erase thermal history. A more detailed description of DMS procedures can be found elsewhere.[19]

III. Results and Analysis

Twenty-eight ISO/I, ISO/S, and ISO/I/S blends were prepared with overall compositions (i.e., block copolymer plus homopolymer) at or close to those associated with the three network phases identified in our previous reports describing neat ISO triblocks.[20,21] Table 2 lists the blend compositions studied during this work, bounded by $0.19 \le f_I \le 0.49$, $0.33 \le f_S \le 0.63$, and $0.13 \le f_O \le 0.27$. Figure 1 locates these blends on a ternary phase portrait along with a summary of the neat triblock phase behavior. Blend phase behavior was determined based on a combination of SAXS, TEM, birefringence, and DMS experiments. Three network phases were documented, Q^{230}, O^{70}, and Q^{214}, along with two order−order transitions, $O^{70} \leftrightarrow Q^{230*}$ and $Q^{214} \leftrightarrow O$,[70] where Q^{230*} refers to a double gyroid phase located at a previously unreported composition.[20,21]

At this point we must emphasize that the classification of ISO morphologies as "two-domain" and "three-domain" can be misleading. All our results correspond to a state of intermediate segregation strength, with smoothly varying periodic composition fields, the symmetry of which define the morphology. Thus, for any single morphology that stretches continuously from a two-domain diblock limit, there is no simple way to determine at which point a third domain exists. In principle, our deduced symmetries (with the exception of $I4_132$) can support two or three domains. Even with diblock copolymers, there is ambiguity in identifying the number of domains (1 or 2). For example, a fluctuating disordered state is nearly as "two-domain" as an ordered phase near the ODT. Lodge and others have dealt with the identification of discrete polymer domains, emphasizing how ambiguous this analysis can be.[44,45]

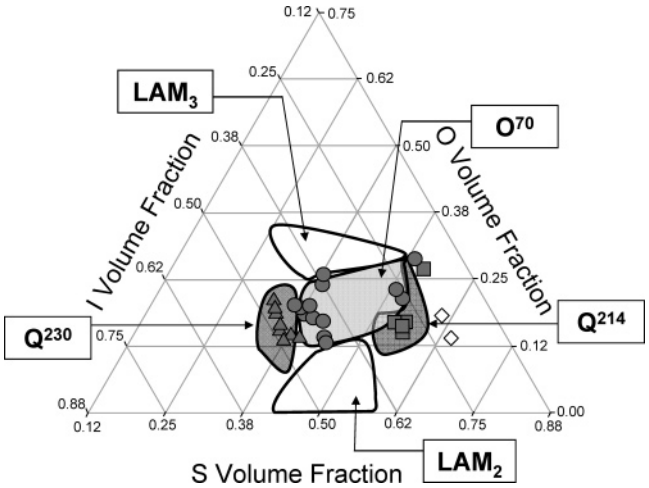

Figure 1. Poly(isoprene) [I], poly(styrene) [S], and poly(ethylene oxide) [O] ternary volume fraction phase portrait. Five labeled areas (LAM_3, LAM_2, Q^{230}, O^{70}, Q^{214}) identify regions of neat ISO triblock copolymer phase behavior near the order−disorder transition, as reported in refs 20 and 21. Blend samples (ISO/I, ISO/S, and ISO/I/S) are indicated by the symbols, where the shape corresponds to the blend morphology: ▲, Q^{230}; ●, O^{70}; ■, Q^{214}. These symbols indicate the lowest temperature structure in samples exhibiting an order−order transition. Open symbols represent samples disordered at all temperatures above 100 °C.

Single Phases. Most of the mixtures studied are situated at compositions between regions of two- and three-domain lamellae (LAM_2 and LAM_3, respectively). Ordered and disordered blends are identified with filled and open symbols, respectively (Figure 1). In this section we describe how each of these morphologies was characterized.

Figure 2 and Figure 3 display representative one-dimensional APS-SAXS data (intensity vs q) from neat triblocks and triblock/homopolymer blends located in the I-rich portion of the phase triangle. Figure 2 deals with ISO-2a (Table 1) and blend B1 (see Table 2), both at 160 °C. A series of reflections are evident in Figure 2a, with relative wavevector positions $\sqrt{6}q/q^*$: $\sqrt{6}$, $\sqrt{8}$, $\sqrt{14}$, $\sqrt{16}$, $\sqrt{20}$, $\sqrt{22}$, $\sqrt{24}$, and $\sqrt{26}$. This familiar sequence uniquely defines the $Ia\bar{3}d$ space group, and we further associate this scattering pattern with the pentacontinuous Q^{230} double gyroid morphology based on the approximate 10-fold intensity ratio between the first (112) and second (022) reflections,[14,46] along with TEM, differential scanning calorimetry (DSC), and modeling results reported previously.[20,21]

Blending 11.7 vol % poly(styrene) homopolymer with ISO-2a (blend B1) leads to a qualitatively different SAXS pattern, shown in Figure 2b. The sequence of Bragg reflections cannot be indexed with space groups commonly found in ordered block copolymers, e.g., cubic, hexagonal, or lamellae. However, an orthorhombic Bravais lattice, with space group *Fddd* (no. 70), does accommodate this diffraction pattern, and the associated allowed reflections are identified in Figure 2b. This result mirrors what we reported earlier for neat ISO triblock copolymer melts at similar compositions.[20,21] On the basis of our previous analysis, and the similarity in SAXS peak positions and intensities, we deduce that blend B1 contains the triply continuous O^{70} network morphology. Diffraction peaks in blends B4, B5, B6, B7, B8, and B9 support the O^{70} phase assignment, as well (see Table 2).

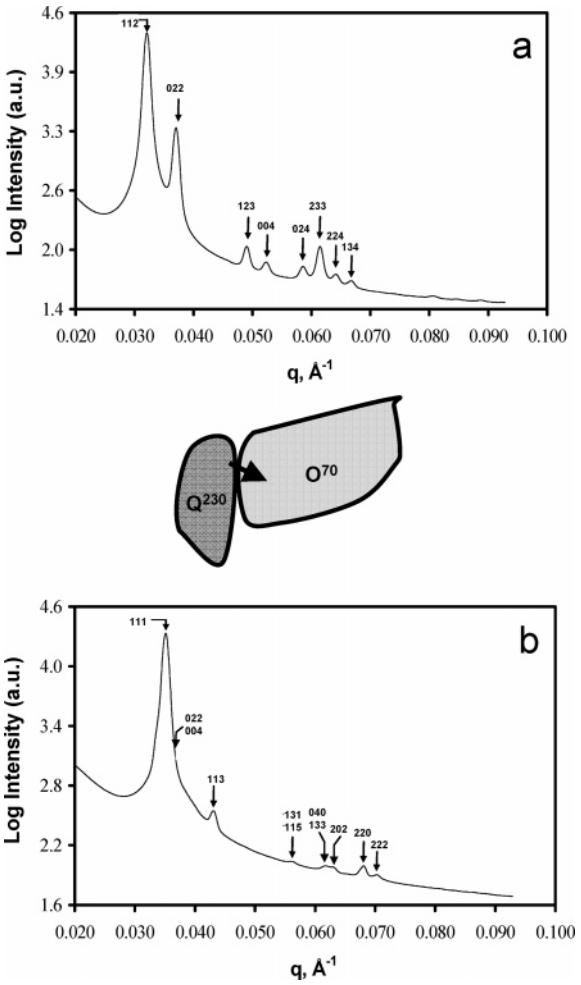

Figure 2. (a) APS-SAXS data for ISO-2a (0.49/0.36/0.15) indexed according to the $Ia\bar{3}d$ space group and consistent with the Q^{230} network phase. (b) APS-SAXS data for B1 (0.43/0.44/0.13), a blend of ISO-2a, and poly(styrene) homopolymer. Peaks are indexed according to the *Fddd* space group, and this specimen is assigned the O^{70} network phase. The center sketch shows the change in composition in Figure 1 upon blending.

APS-SAXS data obtained from neat triblock ISO-3g at 160 °C also contain reflections that are consistent with the O^{70} phase assignment (see Figure 3a and ref 21). A different SAXS pattern emerges when this polymer is blended with 10.9 vol % poly(isoprene) homopolymer (blend B11), as shown in Figure 3b. This pattern is nearly identical to that seen in Figure 2a; hence, we conclude that blend B11 has $Ia\bar{3}d$ space group symmetry, and the sample is assigned the Q^{230} morphology. Several blends listed in Table 1 showed similar behavior, including B10, B12, and B13. In all cases, blending either I or S homopolymer on the I-rich side of the phase triangle results in SAXS patterns identical to those of the pure ISO materials at the corresponding overall compositions (see Figure 1).

Figures 4 and 5 contain APS-SAXS patterns recorded from two triblocks and two blends located in the S-rich portion of the phase triangle. Figure 4a shows SAXS results obtained at 160 °C from ISO-16d. This pattern, similar to those found in Figures 2b and 3a, was shown earlier to arise from the O^{70} morphology.[21] Mixing ISO-16d with 17.4 vol % poly(styrene) homopolymer (blend B18) produces the data shown in Figure 4b. Scattering peaks found at position $\sqrt{2}q/q^*$ of $\sqrt{2}$, $\sqrt{6}$, $\sqrt{8}$, $\sqrt{12}$, $\sqrt{14}$, $\sqrt{16}$, and $\sqrt{20}$ are indicative of cubic

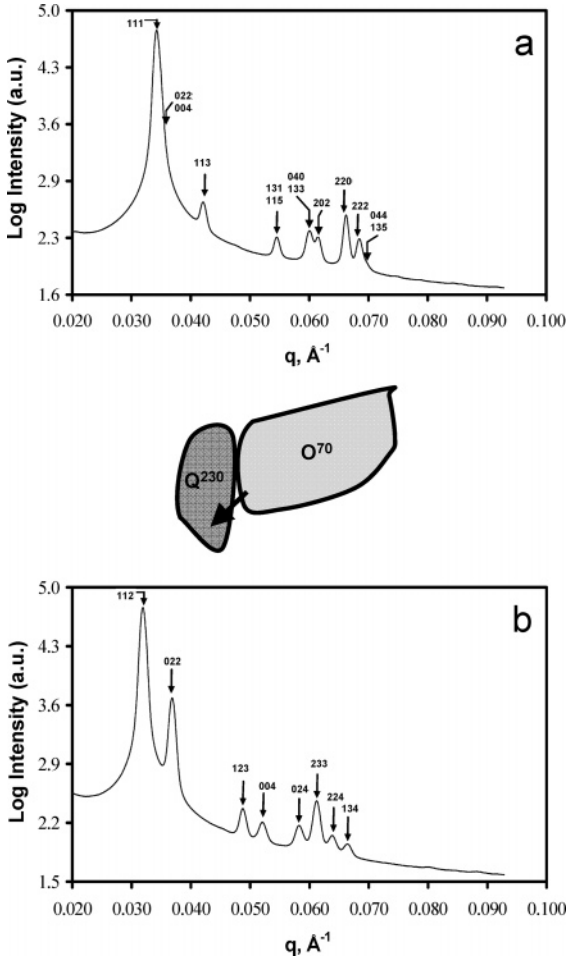

Figure 3. (a) APS-SAXS data for ISO-3g (0.41/0.41/0.18). Peaks are indexed according to the *Fddd* space group, consistent with the O^{70} network morphology. (b) APS-SAXS data for B11 (0.48/0.36/0.16), a blend of ISO-3g, and poly(isoprene) homopolymer. Peaks are indexed based on the $Ia\bar{3}d$ space group, and this specimen is assigned the Q^{230} network phase. The center sketch shows the composition change in Figure 1 upon blending.

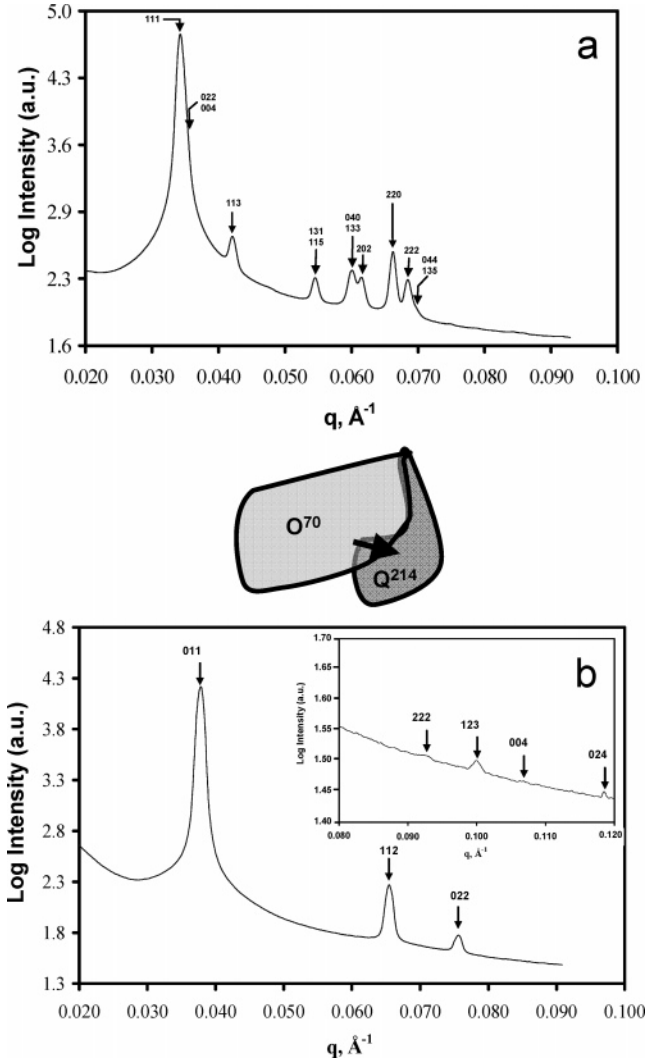

Figure 4. (a) APS-SAXS data for ISO-16d (0.35/0.44/0.21). The peaks are indexed according to the *Fddd* space group consistent with the O^{70} network phase. (b) APS-SAXS data for B18 (0.29/0.054/0.17), a blend of ISO-16d, and poly(styrene) homopolymer. Peaks are indexed according to the $I4_132$ space group with higher order reflections shown in the inset. This symmetry is indicative of the Q^{214} network phase. The center sketch shows the change in location in Figure 1 upon blending.

order. Absence of a reflection at the $\sqrt{4}$ position eliminates all but the $I4_132$ space group, which leads to the indexing scheme identified in Figure 4b. As described previously,[21] this assignment is consistent with the triply periodic alternating gyroid phase denoted Q^{214}. Another blend displaying this scattering signature is B20 (see Table 2).

Figure 5a shows SAXS data obtained from ISO-1a at 90 °C. This scattering pattern is similar to the one found in Figure 4b and is assigned the alternating gyroid (Q^{214}) morphology. Scattering peaks are found at position $\sqrt{2}q/q^*$ of $\sqrt{2}$, $\sqrt{6}$, $\sqrt{8}$, $\sqrt{10}$, $\sqrt{12}$, $\sqrt{14}$, $\sqrt{16}$, and $\sqrt{20}$, indicative of cubic order. Again, absence of a reflection at the $\sqrt{4}$ position eliminates all but the $I4_1$-32 space group. Mixing this triblock copolymer with 14.6 vol % poly(isoprene) (blend B14) leads to the SAXS pattern shown in Figure 5b, recorded at 90 °C (SAXS data for Figure 5 were collected at 90 °C, as opposed to the 160 °C in Figures 2−4, due to the T_{ODT}'s of ISO-1a [166 °C] and B14 [160 °C]). On the basis of the similarity with Figures 3a and 4a, we have indexed this sequence of reflections in Figure 5b as *Fddd* and assigned the O^{70} phase to this material. As with the I-rich side of the channel of network phases, morphologies created by blending S or I homopolymer on the S-rich side of this region map directly onto the phase triangle associated with the neat ISO polymers (see Figure 1), except as noted below.

Figures 2−5 illustrate network-to-network transitions induced by doping neat triblock copolymer with either S or I homopolymer. The O^{70} network phase was also formed by blending both S and I homopolymers with ISO-3k and ISO-3l (blends B27 and B28, respectively). Figure 6a illustrates an IT-SAXS scattering pattern taken from ISO-3k at 160 °C. Peak intensities at relative q spacings of q^* and $2q^*$ along with previous work on this sample indicate a three-domain lamellar (LAM$_3$) morphology.[21] Addition of 7.6 vol % poly(styrene) homopolymer and 6.8 vol % poly(isoprene) homopolymer to ISO-3k at 160 °C (blend B27) produces the SAXS data displayed in Figure 6b. Because of lower instrument resolution and less X-ray flux associated with the IT-SAXS machine, the Bragg reflections in Figure 6 are broader and the signal-to-noise ratio is lower than the corresponding data in Figures 2−5 (APS-SAXS). Nevertheless, the pattern of peaks found in Figure 6b is characteristic of the O^{70} phase as described else-

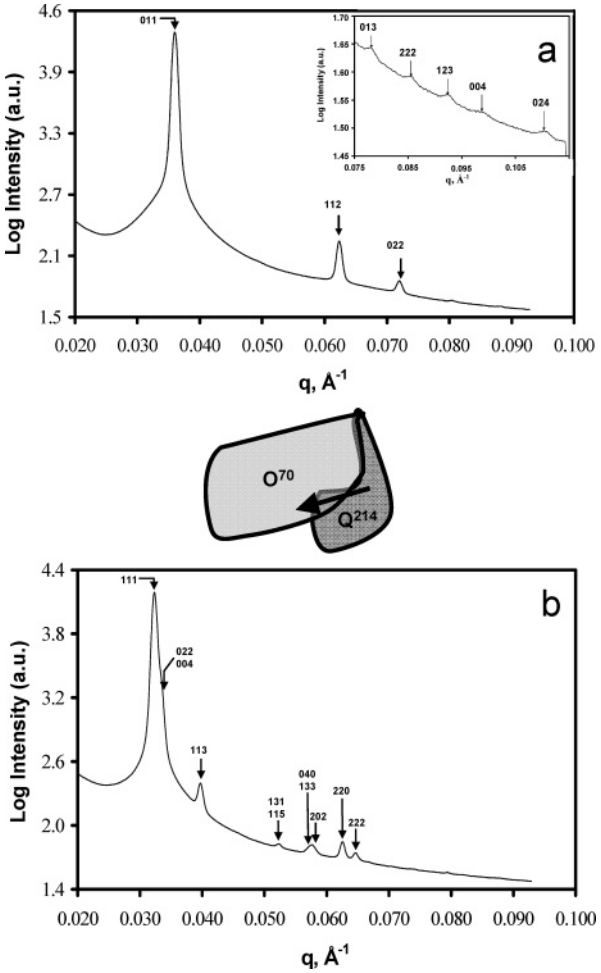

Figure 5. (a) APS-SAXS data for neat ISO-1a (0.32/0.51/0.17) at 90 °C. Peaks are indexed according to the $I4_132$ space group characteristic of the Q^{214} morphology. (b) APS-SAXS data (90 °C) for B14 (0.43/0.43/0.14), a blend of ISO-1a, and poly(isoprene) homopolymer. Peaks are indexed according to the *Fddd* space group, consistent with the O^{70} network phase. The center sketch shows the change in composition in Figure 1 upon blending.

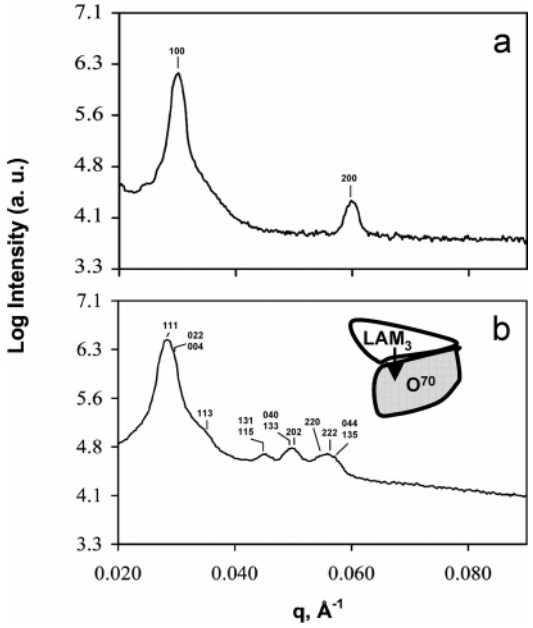

Figure 6. IT-SAXS data for (a) ISO-3k (0.36/0.37/0.27) and (b) B27 (0.34/0.40/0.26), a blend of ISO-3k and poly(styrene) and poly(isoprene) homopolymer. Both specimens were annealed at 200 °C for 15 min, then cooled to 160 °C, and held at that temperature for 30 min prior to X-ray exposure. Relative peak positions in (a) are consistent with a lamellar morphology, while the scattering pattern in (b) is consistent with the O^{70} phase. All the *Fddd* reflections indicated in (b) cannot be resolved with the IT-SAXS instrument. However, as shown elsewhere,[19] this scattering pattern is a fingerprint for the O^{70} structure. The sketch identifies the change in composition in Figure 1 upon blending.

where.[19,21] In particular, the three broad rounded peaks occurring over $0.04 < q < 0.06$ Å^{-1} correspond to the convolution of the (131) and (115), (040) and (133), (202), (220), (222), and (004), and (135) reflections that are resolved in Figures 2b, 3a, 4a, and 5b.

In every instance reported here the blended specimens produced SAXS patterns with an equivalent number of, and nearly equally well-defined, diffraction peaks as were obtained from pure ISO melt materials (with the same morphology), indicative of comparable degrees of long-range order. Two other types of experiment were employed to corroborate this conclusion. TEM images were obtained from microtomed and OsO_4 stained specimens. Representative images taken from blends B3, B4, and B18, which were assigned the Q^{230}, O^{70}, and Q^{214} morphologies based on SAXS analysis, respectively, are shown in Figure 7. These pictures are presented primarily to illustrate the preservation of translational order upon doping with homopolymer; a more complete analysis of similar TEM images was presented in an earlier publication.[21]

Slowly cooling a block copolymer melt slightly below T_{ODT}, where conversion from disorder to order is governed by nucleation events, can lead to the formation of relatively few large ordered grains. SAXS patterns from small volumes of such samples (e.g., obtained with a small diameter X-ray beam and a thin specimen) will contain scattering attributable to individual "single crystals". Figure 8 illustrates such a result, obtained after cooling blend B14 from 170 to 150 °C over a period of 8 h, where $T_{ODT} = 160$ °C. Individual diffraction spots are indexed according to the *Fddd* space group, derived from powder pattern scattering (see Figure 5b) and based on our previous comprehensive analysis of the O^{70} phase.[21] Agreement between the experimental and calculated peak positions for a subset of the recorded diffraction data, including the azimuthal angle dependence, reinforces our space group assignment and corroborates our conclusion regarding long-range order.

Order−Order Transitions. Most of the ISO triblock copolymers examined in our previous reports exhibited a single ordered phase between 100 and 200 °C.[21] However, in several samples a $Q^{214} \leftrightarrow O^{70}$ network-to-network phase transition was documented at compositions situated at the boundary between these ordered states (see Figure 1). We have identified this order−order transition (OOT) along with a second network-to-network transition in certain blend specimens as described in this section.

Figure 9 shows IT-SAXS powder patterns recorded at 90 and 130 °C from blend B25. On the basis of the SAXS analyses described in the previous section, the low- and high-temperature ordered states are consistent with Q^{214} and O^{70} phase assignments, respectively (see Figures 4b and 5b). Figure 10 shows a light depolarization (birefringence) experiment conducted while cooling (1 °C/min) this material from 175 to 85 °C. An intermediate optically active state separates two optically isotropic regions, consistent with a sequence of

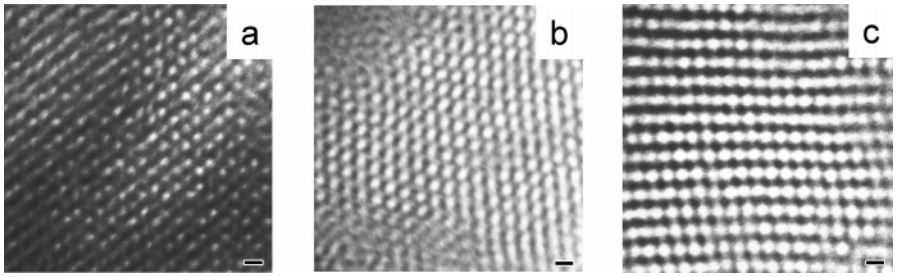

Figure 7. TEM images obtained from (a) blend B3 (Q^{230} based on SAXS), (b) blend B4 (O^{70} based on SAXS), and (c) blend B18 (Q^{214} based on SAXS). Thin sections were stained with OsO_4 to enhance the contrast. All three micrographs confirm the presence of long-range order in blends of ISO triblock copolymer with I or S homopolymer. Three-fold (a) and four-fold (c) projections are consistent with the Q^{230} and Q^{214} cubic phase assignments, respectively. The image in (b) is consistent with a network morphology. Scale bars represent 30 nm.

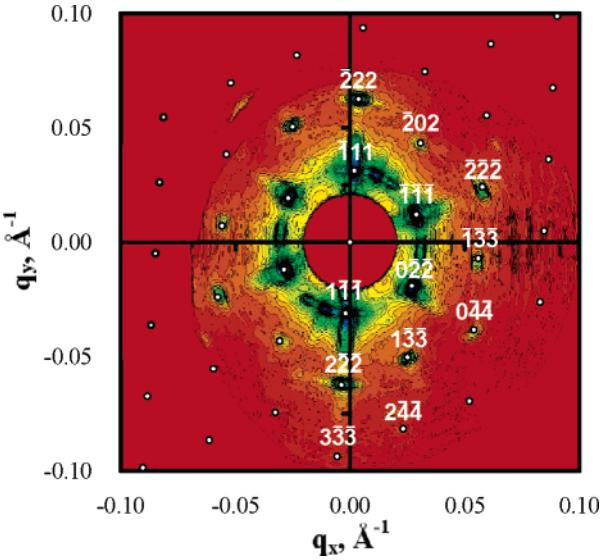

Figure 8. 2-D SAXS pattern obtained from blend B14 after slow cooling from 170 to 150 °C over a period of 8 h, where T_{ODT} = 160 °C. Nucleation limited growth of the O^{70} phase results in the formation of few relatively large grains, which produce single-crystal diffraction. Indexing with the *Fddd* space group accounts for a significant number of the reflections as indicated by the white spots and numbers. This data set was acquired with the IT-SAXS instrument.

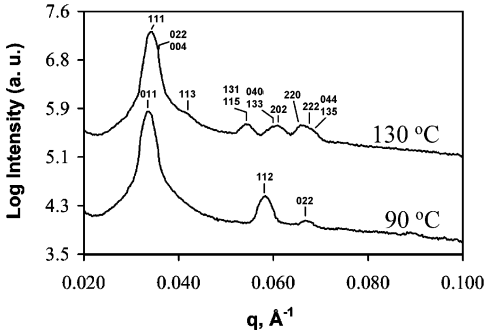

Figure 9. IT-SAXS data recorded for blend B25 at 90 and 130 °C. The sample was heated to 200 °C, annealed for 15 min and then cooled to 90 °C, held for 1 h and measured, then heated to 130 °C, held for 1 h, and measured again. The upper curve (130 °C) is indexed according to the orthorhombic *Fddd* space group. The lower curve (90 °C) is indexed according to the cubic $I4_132$ space group. The curves are shifted vertically for clarity.

three phases: disorder ↔ O^{70} ↔ Q^{214} with T_{ODT} = 135 °C and T_{OOT} = 107 °C (only cooling data are shown in Figure 10). This blend phase behavior mimics the thermodynamic properties of pure triblock specimens ISO-15b and ISO-15e as reported earlier.[21]

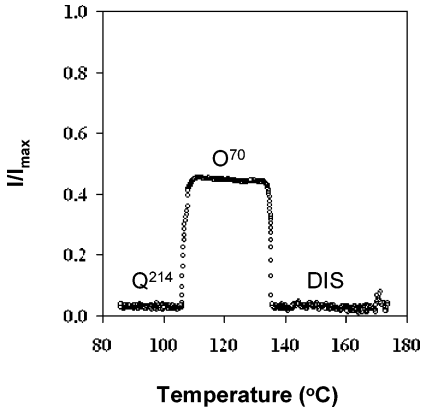

Figure 10. Light depolarization intensities obtained while cooling blend B25. Birefringence at intermediate temperatures is consistent with orthorhombic (O^{70}) symmetry, while the absence of optical activity at higher and lower temperatures supports assignments of disordered (DIS) and cubic (Q^{214}) states, respectively.

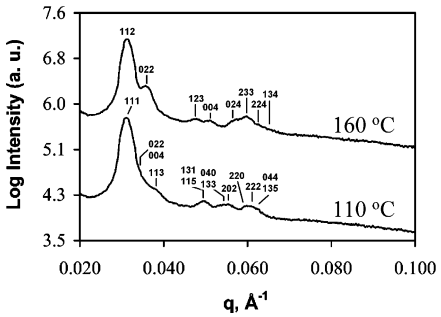

Figure 11. IT-SAXS data obtained from blend B26 at 110 and 160 °C. The sample was heated to 200 °C, annealed for 15 min and then cooled to 110 °C, held for 1 h and measured, then heated to 160 °C, held for 1 h, and measured again. The upper curve (160 °C) is indexed according to the *Ia*3*d* space group, consistent with a double gyroid morphology. The lower curve (110 °C) is indexed according to the orthorhombic *Fddd* space group and is consistent with the O^{70} morphology. The curves are shifted vertically for clarity.

Three other blends, B21, B22, and B26, displayed sets of low- and high-temperature SAXS and birefringence patterns indicative of distinctly different ordered phases. We illustrate these properties using SAXS (Figure 11) and birefringence (Figure 12) data obtained from blend B26. Analogous to our analysis of Figures 6b and 9, we associate the 110 °C SAXS pattern in Figure 11 with the O^{70} phase. Heating the material to 160 °C transforms the X-ray scattering response to a pattern consistent with the cubic double gyroid morphology. Birefringence measurements recorded while cooling (1 °C/min) blend B26 (see Figure 12) are consistent with these

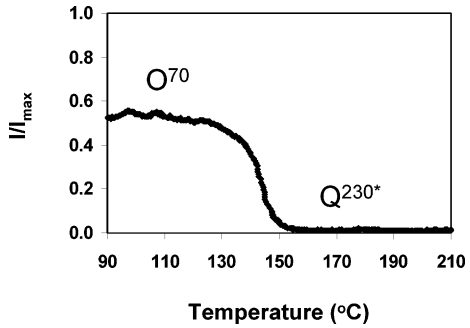

Figure 12. Light depolarization intensities obtained while cooling blend B26. Optical activity at lower temperatures is consistent with orthorhombic symmetry, while the absence of optical activity at higher temperatures supports the $Ia\bar{3}d$ cubic assignment.

assignments, where the $Q^{230*} \rightarrow O^{70}$ transition occurs on cooling at about $T_{OOT} \cong 143$ °C. Because we cannot discriminate between the pentacontinuous ("three-color") and tricontinuous ("two-color") versions of the double gyroid structure based on SAXS data alone, we refer to this phase as Q^{230*}. In this case TEM analysis of the $Ia\bar{3}d$ structure was not performed, as the structure was the higher temperature phase in an OOT. Also, T_{ODT} (disorder $\rightarrow Q^{230*}$) could not be located using the birefringence technique because both states are optically isotropic. T_{ODT} was greater than the upper limit of the SAXS apparatus [200 °C]. We return to these network-to-network transitions in the Discussion section.

IV. Discussion

The results presented in the previous section demonstrate how small to modest amounts of homopolymer (up to 21 vol %) influence the phase behavior of ISO triblock copolymers in the vicinity of the multicontinuous network phases. In general, our findings are consistent with the extensive literature dealing with AB diblock and ABA triblock copolymers when mixed with A and/or B homopolymers, when the homopolymer molecular weights are equal to or less than the corresponding block molecular weights.[30,32,34,35] As Figure 1 summarizes, well-ordered Q^{230}, O^{70}, and Q^{214} network phases can be formed by blending ISO triblocks with either or both I and S homopolymer, where the resulting morphological behavior coincides with the pure triblock copolymer phase portrait.

These findings have both fundamental and practical significance. Blending offers an efficient strategy for exploring block copolymer phase behavior, particularly when the number of composition variables increases, accompanied by an expansion in the portfolio of known and unknown ordered phases. Synthesizing all the block copolymers necessary to fully characterize pure triblock phase behavior represents an exhausting and time-consuming exercise. Moreover, as more phases are located within a finite composition window, this approach becomes impractical notwithstanding effort; uncertainties in composition and molecular weight, inevitable byproducts of the synthesis, and characterization methods become limiting factors. Modest amounts of homopolymer offer precise and continuous control over the composition variables, making the characterization of complex phase behavior much more tractable. This approach, already exploited with two-monomer block copolymers,[24−26,35,36] will be valuable in mapping experimental phase behavior in multiblock systems. Blending also may be useful in developing network phases for practical purposes. In the event that network symmetry influences an application property (e.g., birefringence) the material could be transformed between two mechanically equivalent morphologies by appropriate doping with small amounts of homopolymer.

Our results indicate that the phase behavior can be modified by expanding either the poly(isoprene) domains or the poly(styrene) domains, or both. Homopolymer addition to either domain type generally leads to predictable phase transitions with SAXS patterns and TEM images that reflect long-range order comparable to that obtained with the pure ISO materials. That both types of homopolymer lead to well-defined Q^{230}, O^{70}, and Q^{214} phases suggests that these networks are rather stable thermodynamically. As noted in our earlier report,[21] we believe the local trivalent connector geometry in the three network phases represents a robust building block for morphology formation in linear block copolymers.

Identification of a new order−order transition, $O^{70} \leftrightarrow Q^{230*}$, on the styrene-rich side of the network channel indicates a subtle but significant impact of homopolymer near the phase boundaries. On the basis of the pure ISO results, we would not expect to find the double gyroid near the Q^{214} phase. However, all three examples of the $O^{70} \leftrightarrow Q^{230*}$ transition involve addition of S homopolymer. As discussed in the Introduction, homopolymer can be mixed with end blocks by either swelling the blocks (wet brush) or intercalating into the center of the domains (dry brush).[40,41] Mixing S homopolymer with ISO in the dry brush limit presents a packing dilemma since a three-domain morphology requires all the S blocks to bridge I and O domains. (We rule out the possibility of lateral separation of S homopolymer from S blocks since this would place severe packing constraints on the I and O blocks.) We suspect this domain packing problem leads to the $O^{70} \leftrightarrow Q^{230*}$ phase transition. Although we cannot discriminate between two- and three-domain versions of the gyroid phase based solely on SAXS data, we believe the Q^{230*} morphology corresponds to the former. That is, the problem of packing S homopolymer into a three-domain morphology is rectified by creation of a two-domain gyroid state (e.g., I plus mixed S and O domains or O plus mixed I and S).

This hypothesis is supported by the phase state identified in blends B23 and B24 (Table 2). Both of these mixtures formed by adding S homopolymer to network forming ISO-15a and ISO-15b (see Table 1) are disordered at 100 °C, as shown in Figure 1. Obviously, the homopolymer destabilizes the ordered state. This trend is consistent with the reduction in segregation, from three to two domains, which we suggest occurs with the Q^{230*} phase.

Again we must emphasize that the classification of ISO morphologies as "two-domain" and "three-domain" can be misleading. All our results correspond to a state of intermediate segregation strength, with composition profiles that are unlikely to saturate at bulk densities anywhere within the segregated domains. Thus, for any single morphology that stretches continuously from a two-domain diblock limit, there is no simple way to determine at which point a third domain exists. For example, assuming $\chi_{AB}N = \chi_{BC}N = 13$ and $\chi_{AC}N = 35$, Tyler and Morse have calculated that an ABC triblock copolymer exhibits a lamellar morphology along the entire $f_A = f_B = 1/2$ isopleth for $0 \leq f_C \leq 1/3$.[22] Obviously,

the $f_C = 0$ (diblock) case is a two-domain structure, and the $f_C = 1/3$ material will reflect three equally segregated domains. Thus, the transition between these two limiting cases is continuous since there is not a change in symmetry. As illustrated in Figure 1, the O^{70} phase separates what we refer to as LAM_2 and LAM_3, making the distinctions less ambiguous. However, characterization of any ordered phase that may stretch continuously from the diblock limit into the three-domain region will be subject to this qualification.

We believe that Q^{230*} may fall into this category. Theory indicates that a channel of double gyroid morphology should extend from the $f_I = 0$ axis (i.e., SO diblock)[22] up to roughly where we have identified Q^{230*}. Presumably, the added constraints associated with swelling the center S block with homopolymer also can induce this behavior. Additional experimental and theoretical work will be necessary to verify these arguments.

V. Conclusions

Ordered state phase behavior has been investigated in poly(isoprene-*b*-styrene-*b*-ethylene oxide) (ISO) triblock copolymers mixed with I and/or S homopolymer, where the homopolymer molecular weights are similar to the corresponding block molecular weights. Using small-angle X-ray scattering (SAXS), transmission electron microscopy (TEM), dynamic mechanical spectroscopy (DMS), and birefringence measurements, we have shown how modest concentrations of homopolymer (up to 21 vol %) can be used to switch between the network phases Q^{230} and O^{70}, O^{70} and Q^{214}, and between O^{70} and three-domain lamellae. Blending has little impact on the location in composition space of the network phases relative to the neat ISO triblocks. TEM and SAXS data also demonstrate that the degree of long-range order found in the neat triblock materials is preserved in the triblock copolymer/homopolymer blends considered in this study. A heretofore unreported transition from O^{70} to Q^{230*} was identified upon heating several ISO/S blends. We tentatively identify the Q^{230*} state as two-domain double gyroid and attribute this behavior to packing frustration associated with mixing homopolymer with the center S block.

These experiments demonstrate an efficient strategy for controlling morphology in three-domain ordered block copolymer systems, thereby relaxing the synthetic demands associated with preparing new compositions. Blending ABC triblock copolymers with homopolymers offers a practical approach to searching for new morphologies in the complex field of multiblock copolymers. We are particularly enthusiastic about the prospects for evaluating the results of self-consistent mean-field theory in this way.

Acknowledgment. This work was supported by the NSF through Grant DMR-0220460. A Graduate fellowship to T.H.E. from Lucent Technologies is gratefully acknowledged. The authors thank Ryan Waletzko for his help in synthesizing several of the polymers investigated in this work. Use of the Advanced Photon Source at Argonne National Labs was supported by the U.S. Department of Energy, Basic Energy Sciences, Office of Science, under Contract W-31-109-Eng-38. This research program has made extensive use of the MRSEC (NSF) supported Institute of Technology Characterization Facility at the University of Minnesota, Twin Cities Campus.

References and Notes

(1) Edrington, A. C.; Urbas, A. M.; DeRege, P.; Chen, C. X.; Swager, T. M.; Hadjichristidis, N.; Xenidou, M.; Fetters, L. J.; Joannopoulos, J. D.; Fink, Y.; Thomas, E. L. *Adv. Mater. (Weinheim, Ger.)* **2001**, *13*, 421−425.
(2) Finnefrock, A. C.; Ulrich, R.; Toombes, G. E. S.; Gruner, S. M.; Wiesner, U. *J. Am. Chem. Soc.* **2003**, *125*, 13084−13093.
(3) Gruner, S. M. *Proc. SPIE-Int. Soc. Opt. Eng.* **1996**, *2716* (Smart Materials Technologies and Biomimetics), 309−312.
(4) Park, M.; Harrison, C.; Chaikin, P. M.; Register, R. A.; Adamson, D. H. *Science (Washington, D.C.)* **1997**, *276*, 1401−1404.
(5) Urbas, A. M.; Maldovan, M.; DeRege, P.; Thomas, E. L. *Adv. Mater. (Weinheim, Ger.)* **2002**, *14*, 1850−1853.
(6) Kim, S. O.; Solak, H. H.; Stoykovich, M. P.; Ferrier, N. J.; de Pablo, J. J.; Nealey, P. F. *Nature (London)* **2003**, *424*, 411−414.
(7) Rzayev, J.; Hillmyer, M. A. *Macromolecules* **2005**, *38*, 3−5.
(8) Davidock, D. A.; Hillmyer, M. A.; Lodge, T. P. *Macromolecules* **2003**, *36*, 4682−4685.
(9) Floudas, G.; Vazaiou, B.; Schipper, F.; Ulrich, R.; Wiesner, U.; Iatrou, H.; Hadjichristidis, N. *Macromolecules* **2001**, *34*, 2947−2957.
(10) Khandpur, A. K.; Foerster, S.; Bates, F. S.; Hamley, I. W.; Ryan, A. J.; Bras, W.; Almdal, K.; Mortensen, K. *Macromolecules* **1995**, *28*, 8796−806.
(11) Matsen, M. W.; Bates, F. S. *Macromolecules* **1996**, *29*, 1091−1098.
(12) Zhao, J.; Majumdar, B.; Schulz, M. F.; Bates, F. S.; Almdal, K.; Mortensen, K.; Hajduk, D. A.; Gruner, S. M. *Macromolecules* **1996**, *29*, 1204−1215.
(13) Bailey, T. S.; Pham, H. D.; Bates, F. S. *Macromolecules* **2001**, *34*, 6994−7008.
(14) Shefelbine, T. A.; Vigild, M. E.; Matsen, M. W.; Hajduk, D. A.; Hillmyer, M. A.; Cussler, E. L.; Bates, F. S. *J. Am. Chem. Soc.* **1999**, *121*, 8457−8465.
(15) Hueckstaedt, H.; Goldacker, T.; Goepfert, A.; Abetz, V. *Macromolecules* **2000**, *33*, 3757−3761.
(16) Suzuki, J.; Seki, M.; Matsushita, Y. *J. Chem. Phys.* **2000**, *112*, 4862−4868.
(17) Matsen, M. W. *J. Chem. Phys.* **1998**, *108*, 785−796.
(18) Cochran, E. W.; Bates, F. S. *Phys. Rev. Lett.* **2004**, *93*, 087802.
(19) Bailey, T. S.; Hardy, C. M.; Epps, T. H., III; Bates, F. S. *Macromolecules* **2002**, *35*, 7007−7017.
(20) Epps, T. H., III; Cochran, E. W.; Hardy, C. M.; Bailey, T. S.; Waletzko, R. S.; Bates, F. S. *Macromolecules* **2004**, *37*, 7085−7088.
(21) Epps, T. H., III; Cochran, E. W.; Bailey, T. S.; Waletzko, R. S.; Hardy, C. M.; Bates, F. S. *Macromolecules* **2004**, *37*, 8325−8341.
(22) Tyler, C. A.; Morse, D. C. *Phys. Rev. Lett.* **2005**, *94*, 208302.
(23) Hillmyer, M. A.; Bates, F. S. *Macromolecules* **1996**, *29*, 6994−7002.
(24) Janert, P. K.; Schick, M. *Macromolecules* **1998**, *31*, 1109−1113.
(25) Matsen, M. W. *Macromolecules* **1995**, *28*, 5765−5773.
(26) Matsen, M. W. *Phys. Rev. Lett.* **1995**, *74*, 4225−4228.
(27) Laurer, J. H.; Hajduk, D. A.; Dreckoetter, S.; Smith, S. D.; Spontak, R. J. *Macromolecules* **1998**, *31*, 7546−7549.
(28) Goldacker, T.; Abetz, V.; Stadler, R.; Erukhimovich, I.; Leibler, L. *Nature (London)* **1999**, *398*, 137−139.
(29) Abetz, V.; Goldacker, T. *Macromol. Rapid Commun.* **2000**, *21*, 16−34.
(30) Bodycomb, J.; Yamaguchi, D.; Hashimoto, T. *Macromolecules* **2000**, *33*, 5187−5197.
(31) Goldacker, T.; Abetz, V.; Stadler, R. *Macromol. Symp.* **2000**, *149* (6th European Symposium on Polymer Blends, 1999), 93−98.
(32) Sugiyama, M.; Shefelbine, T. A.; Vigild, M. E.; Bates, F. S. *J. Phys. Chem. B* **2001**, *105*, 12448−12460.
(33) Dotera, T. *Phys. Rev. Lett.* **2002**, *89*, 205502/1−205502/4.
(34) Suzuki, J.; Furuya, M.; Iinuma, M.; Takano, A.; Matsushita, Y. *J. Polym. Sci., Part B: Polym. Phys.* **2002**, *40*, 1135−1141.
(35) Floudas, G.; Hadjichristidis, N.; Stamm, M.; Likhtman, A. E.; Semenov, A. N. *J. Chem. Phys.* **1997**, *106*, 3318−3328.
(36) Huh, J.; Jo, W. H. *J. Chem. Phys.* **2002**, *117*, 9920−9926.

(37) Banaszak, M.; Whitmore, M. D. *Macromolecules* **1992**, *25*, 2757−2770.
(38) Likhtman, A. E.; Semenov, A. N. *Macromolecules* **1997**, *30*, 7273−7278.
(39) Xi, H.; Milner, S. T. *Macromolecules* **1996**, *29*, 2404−2411.
(40) Hadjichristidis, N.; Pispas, S.; Floudas, G. A. *Block Copolymers: Synthetic Strategies, Physical Properties, and Applications*; Wiley-Interscience: Hoboken, NJ, 2003.
(41) Hiemenz, P. C. *Polymer Chemistry: The Basic Concepts*; Marcel Dekker: New York, 1984.
(42) Fetters, L. J.; Lohse, D. J.; Richter, D.; Witten, T. A.; Zirkel, A. *Macromolecules* **1994**, *27*, 4639−47.
(43) Rempp, P.; Merrill, E. *Polymer Synthesis,* 2nd ed.; Huthig & Wepf: New York, 1991.
(44) Lodge, T. P.; McLeish, T. C. B. *Macromolecules* **2000**, *33*, 5278−5284.
(45) Shull, K. R.; Mayes, A. M.; Russell, T. P. *Macromolecules* **1993**, *26*, 3929−3936.
(46) Hajduk, D. A.; Harper, P. E.; Gruner, S. M.; Honeker, C. C.; Kim, G.; Thomas, E. L.; Fetters, L. J. *Macromolecules* **1994**, *27*, 4063−4075.

MA050736M